Frequency-doubled Laser System at 780 nm for Pulsed Vapor-cell Clocks

M. Gozzelino*, C.E. Calosso, E.K. Bertacco, F. Levi and S. Micalizio
Quantum Metrology and Nanotechnologies Division
INRIM – Istituto Nazionale di Ricerca Metrologica
Torino, Italy
*m.gozzelino@inrim.it

***Abstract*—We present the development status of a low-noise pulsed laser source suitable for high-performing vapor-cell clocks. The laser is based on a 1560 nm source, frequency doubled to be resonant with the D_2 line of rubidium at 780 nm. The laser system is able to deliver laser pulses with programmable amplitude and length. The intensity noise of the laser during the pulses duration is also actively reduced by means of the same fast analog control loop generating the pulses. The pulses characteristics are shown to be compatible with the specifications of a high-performing Pulsed Optically Pumped (POP) clock.**

***Index Terms*—optical fibers; rubidium; atomic clocks; telecom; GNSS.**

I. Introduction

The performance of laser-pumped vapor-cell clocks strongly relies on the characteristics of the laser source employed [1]–[5]. In particular, the laser intensity noise and the spectral purity can influence the short-term, whereas fluctuations of the mean laser intensity and frequency influence the standard for longer averaging times [6]–[8]. The choice of the laser source is done not only seeking for the lowest noise, but also taking into account the device footprint and power consumption, since vapor-cell clocks are designed to be compact and portable. Expanding the technology diversity of the optical components suitable for Rb clocks is of particular interest, especially for the development of next-generation space-qualified devices [9]. The availability of C-band telecom lasers and of efficient second-harmonic-generation (SHG) crystals at 1560 nm, makes the rubidium spectroscopy addressable with reliable, off-the shelf components [7], [10]. We present a frequency-doubled laser setup able to deliver stable and low-noise programmable pulses resonant with the Rb D_2 transition. The pulses amplitude characteristics is demonstrated to be compatible with the requirements of state-of-the-art Pulsed Optically Pumped (POP) clocks.

II. Laser Setup

The laser setup is depicted in the scheme of Fig. 1. The starting point is the seed laser at 1560.48 nm (Koheras Adjustik C15), with nominal linewidth of 40 kHz, delivering 10 mW of laser power. The seed is amplified by an Erbium-doped fiber amplifier (Koheras Boostik). A fast variable optical attenuator (VOA), based on Microelectromechanical System (MEMS) technology, is used for a double purpose: firstly, to create the pulses for atomic manipulation and detection of the Rubidium atoms; secondly, to stabilize the amplitude of the pulses, reducing the intensity noise (RIN) of the laser source. The laser light is frequency doubled with the use of a Periodically Poled Lithium Niobate (PPLN) waveguide crystal. At the optimal phase-matching temperature (58.5 °C) the crystal has an efficiency:

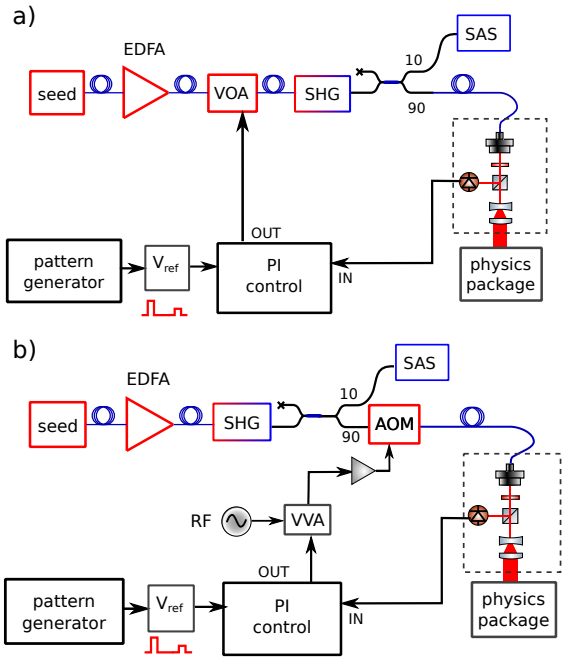

Fig. 1. Scheme of the laser system. a) Pulses generated with the MEMS VOA. b) Pulses generated with a fiber-coupled acousto-optic modulator (AOM) by modulating the RF power with a variable voltage attenuator (VVA). The optics after the collimator include a polarizer, a beam sampler (30 % reflection) and a beam expander. The pick-off beam is acquired with a Si photodiode. EDFA: Erbium-Doped Fiber Amplifier, SHG: Second Harmonic Generation, SAS: Saturation Absorption Setup, PI: Proportional-Integrative

$$\eta/\,(\%/\mathrm{W}) = \frac{P(780\ \mathrm{nm})/\mathrm{W}}{P(1560\ \mathrm{nm})^2/\mathrm{W}^2} \times 100 = 380\,\%/\mathrm{W} \quad (1)$$

This work was partially funded under ESA GSTP contract (Element 2) with Leonardo S.p.A. as prime

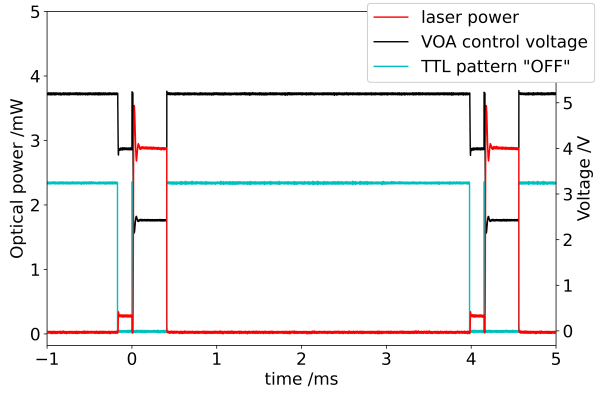

Fig. 2. Optical pulses generated with the active servo-loop. Red: optical power. The smaller pulse is used for the clock "detection" pulse, while the stronger pulse is used for optical pumping. Between the pump and detection pulse the microwave clock interrogation takes place. Black: PI-controller output that drives the control voltage of the VOA. Cyan: one of the two patterns that control the pulses generation ("OFF" phase).

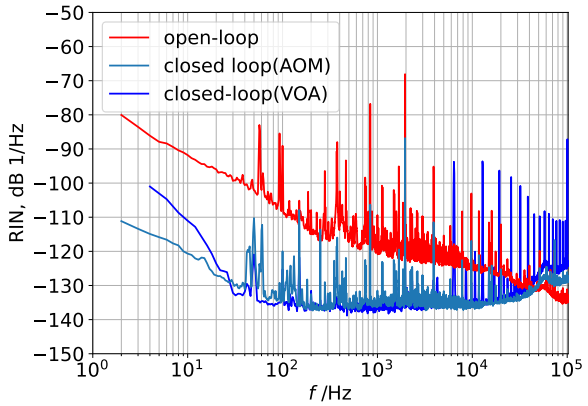

Fig. 3. Relative intensity noise measured at 780 nm. Red: open-loop. Light blue: stabilized with the AOM as actuator ("DET" setpoint). Blue: stabilized with the VOA as actuator ("DET" setpoint). The measurement is performed with the control in CW operation. The measurement is performed with an out-of-loop photodiode.

for input power below $50\,\mathrm{mW}$. At higher pump power, the SHG curve becomes linear with the pump power, with an efficiency $P(780\ \mathrm{nm})/P(1560\ \mathrm{nm}) \simeq 50\,\%$. At operational conditions, we have about $25\,\mathrm{mW}$ output with $80\,\mathrm{mW}$ of input power. The frequency-doubled light is divided by means of a fiber-fused splitter, with $10\,\%$ of the power sent to a saturation-spectroscopy setup for frequency stabilization to a Rb reference cell. The main branch is sent to the proximity of the Rb clock experiment with a fiber patch cord. The beam is collimated, its polarization cleaned with a linear polarizer, and finally expanded to have $\simeq$ 1-cm beam diameter. Prior to the beam-expander, a pick-off beam is extracted for amplitude stabilization.

Since the laser light is pulsed before the SHG unit, pulsed light is sent to the frequency stabilization setup. The low duty cicle ($< 10\,\%$) is currently limiting the frequency-stability achievable with the saturation absorption setup. A fiber-coupled acousto-optic modulator (AOM), operating at 780 nm, is then alternatively employed as actuator (Fig. 1b). This kind of modulator is frequently used for stabilizing intensity fluctuations and it was proven to effectively reduce the RIN and to stabilize the output power for vapor-cells clock applications [11]. Modulating the laser intensity at 780 nm, after the doubling crystal, enables to have CW light for easier frequency stabilization.

The pulses timing is set with two digital patterns coming from the clock control electronics. The amplitude of the pulses commutes between three states: "OFF", "PUMP" and "DET" (for free-evolution, pumping and detection of Rb atoms respectively). The "PUMP" and "DET" power levels are set with two programmable voltage references. During the "OFF" phase the attenuation obtainable in single-pass with the VOA is $30\,\mathrm{dB}$. The extinction ratio becomes more than $50\,\mathrm{dB}$ at 780 nm, thanks to the non-linear response of the doubling crystal. When using the fiber-coupled AOM, the extinction ratio was up to $70\,\mathrm{dB}$.

III. Experimental results

Figure 2 shows the pulses generated with the active control for a typical clock cycle of POP clocks [1]. The pump and detection pulses duration is $0.4\,\mathrm{ms}$ and $150\,\mu\mathrm{s}$ respectively. The rise time is around $5\,\mu\mathrm{s}$ for the detection pulse and $10\,\mu\mathrm{s}$ for the pump pulse respectively.

For the duration of the pulses, the RIN is also stabilized referencing the detected pick-off beam intensity to the low-noise voltage reference. Figure 3 shows the RIN of the fiber laser, as measured just before the physics package on a monitor photodiode in open-loop and when the control is active. Both with the VOA and with the AOM as actuators, the RIN level for the stabilized pulses is below -136 dB 1/Hz for Fourier frequencies in the range from $100\,\mathrm{Hz}$ to $10\,\mathrm{kHz}$, that is the most relevant for typical clock-cycle frequencies [6]. On the basis of the measured noise, the RIN contribution to the POP stability is estimated to be 4×10^{-14} for a detection pulse of $\simeq 200\,\mu\mathrm{s}$.

Another important aspect for clock applications is the pulse area stability. The area of pump and detection pulses affect the clock stability through residual ligh-shift effect [8]. The stability of the pulse area is determined both by the amplitude of the pulses and by the time jitter on the two fronts of the pulse. To estimate the performances of the control in both regards, we performed a syncronous detection of the pulse area. We detected the optical power with a photodiode having a higher bandwidth with respect to the control. Then, the acquired signal is digitized and integrated for a time window spanning the whole pulse duration (plus some margin). The gated detection shares the same clock as the pattern generator feeding the control, thus no timing error is expected from the measurement system. Regarding the amplitude, our measurement system is able to measure fractional stabilities as low as 1×10^{-5}. For both the pumping and detection phases we then measured the area of the pulses and calculated the fractional

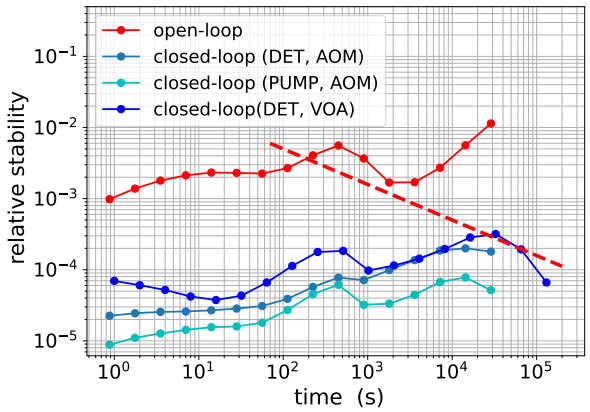

Fig. 4. Fractional stability of the laser-pulses area. Red: open-loop. Blue: detection area with VOA as actuator. Light-blue: detection area with VOA as actuator. Cyan: Pumping area, AOM as actuator. The dashed red line indicates the area stability requirements to obtain $1 \times 10^{-15}\,\tau^{-1/2}$ clock stability for our POP clock.

stability. This is shown in Figure 4. The open loop stability if of a few percent, whereas with the active control was measured to be $< 2 \times 10^{-14}$ for $\tau = 1 \times 10^5\,\mathrm{s}$. This is true both with the AOM and the VOA as actuator. Given the current clock sensitivity, this stability is able to support a clock stability below 1×10^{-15}, thus compatible with the best-performing POP clocks [1]–[4].

The laser system was tested on an engineering model of physics package, designed for the POP operation by Leonardo S.p.A. [9]. Preliminary stability results are shown in Figure 5. The observed short-term stability is $1.2 \times 10^{-13}\tau^{-1/2}$ up to a few thousands seconds averaging time. This is an improvement with comparison to the previous best-reported short-term stability of a laboratory prototype [1], [9]. After removing a linear drift of $+4.6 \times 10^{-14}/\mathrm{d}$, the mid-term stability is well below 1×10^{-14} at one day averaging time, in specifications with next-generation global-navigation-systems clock requirements [12], [13].

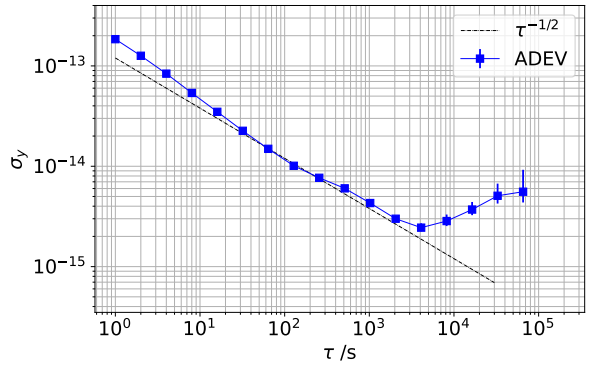

Fig. 5. Fractional stability of the laser-pulses area. $+4.6 \times 10^{-14}/\mathrm{d}$ drift is removed from the whole dataset. The measurement is performed against an active hydrogen maser (7×10^{-14} stability at 1 s and $5 \times 10^{-16}\,\mathrm{d}^{-1}$ drift). Measurement bandwith is 5 Hz.

IV. Conclusion

We reported the development of a fiber-based laser system suitable for the pulsed operation of high-performing vapor-cell clocks. The system is based on a frequency doubled telecom laser, resonant with the rubidium D_2 line. The laser light is pulsed and its intensity stabilized by means of a custom analog control. The laser pulses was characterized in terms of amplitude noise and long-term stability. In both regards, this laser system is able to support the best-performing laser-pumped rubidium clocks. Preliminary tests on a POP Rb clock provided state-of-the-art short-term stability results.

References

[1] S. Micalizio, C. E. Calosso, A. Godone, and F. Levi, "Metrological characterization of the pulsed Rb clock with optical detection," *Metrologia*, vol. 49, pp. 425–436, may 2012.

[2] N. Almat, M. Gharavipour, W. Moreno, F. Gruet, C. Affolderbach, and G. Mileti, "Long-term stability analysis toward <10-14 level for a highly compact POP rb cell atomic clock," *IEEE Trans. Ultrason., Ferroelect., Freq. Contr.*, vol. 67, pp. 207–216, jan 2020.

[3] Q. Shen, H. Lin, J. Deng, and Y. Wang, "Pulsed optically pumped atomic clock with a medium- to long-term frequency stability of 10-15," *Rev. Sci. Instrum.*, vol. 91, p. 045114, apr 2020.

[4] Q. Hao, W. Xue, W. Li, F. Xu, X. Wang, W. Guo, P. Yun, and S. Zhang, "Microwave pulse-coherent technique-based clock with a novel magnetron-type cavity," *IEEE Trans. Ultrason., Ferroelect., Freq. Contr.*, vol. 67, pp. 873–878, apr 2020.

[5] P. Yun, Q. Li, Q. Hao, G. Liu, E. de Clercq, S. Guérandel, X. Liu, S. Gu, Y. Gao, and S. Zhang, "High-performance coherent population trapping atomic clock with direct-modulation distributed bragg reflector laser," *Metrologia*, vol. 58, p. 045001, jul 2021.

[6] C. E. Calosso, M. Gozzelino, A. Godone, H. Lin, F. Levi, and S. Micalizio, "Intensity detection noise in pulsed vapor-cell frequency standards," *IEEE Trans. Ultrason., Ferroelect., Freq. Contr.*, vol. 67, pp. 1074–1079, may 2020.

[7] N. Almat, W. Moreno, M. Pellaton, F. Gruet, C. Affolderbach, and G. Mileti, "Characterization of frequency-doubled 1.5-μm lasers for high-performance Rb clocks," *IEEE Transactions on Ultrasonics, Ferroelectrics, and Frequency Control*, vol. 65, pp. 919–926, jun 2018.

[8] S. Micalizio, A. Godone, F. Levi, and C. Calosso, "Medium-long term frequency stability of pulsed vapor cell clocks," *IEEE Transactions on Ultrasonics, Ferroelectrics and Frequency Control*, vol. 57, pp. 1524–1534, jul 2010.

[9] P. Arpesi, J. Belfi, M. Gioia, N. Marzoli, R. Romani, A. Sapia, M. Gozzelino, C. Calosso, F. Levi, S. Micalizio, A. Tuozzi, and M. Belloni, "Rubidium pulsed optically pumped clock for space industry," in *2019 Joint Conference of the IEEE International Frequency Control Symposium and European Frequency and Time Forum (EFTF/IFC)*, IEEE, apr 2019.

[10] T. Lévèque, L. Antoni-Micollier, B. Faure, and J. Berthon, "A laser setup for rubidium cooling dedicated to space applications," *Appl. Phys. B*, vol. 116, pp. 997–1004, feb 2014.

[11] F. Tricot, D. H. Phung, M. Lours, S. Guérandel, and E. de Clercq, "Power stabilization of a diode laser with an acousto-optic modulator," *Review of Scientific Instruments*, vol. 89, p. 113112, nov 2018.

[12] B. Jaduszliwer and J. Camparo, "Past, present and future of atomic clocks for GNSS," *GPS Solutions*, vol. 25, jan 2021.

[13] S. Micalizio, F. Levi, C. E. Calosso, M. Gozzelino, and A. Godone, "A pulsed-laser Rb atomic frequency standard for GNSS applications," *GPS Solutions*, vol. 25, apr 2021.